agriculture

MDPI

Article

Leaf Carbon and Water Isotopes Correlate with Leaf Hydraulic Traits in Three *Solanum* Species (*S. peruvianum*, *S. lycopersicum* and *S. chilense*)

Diego Barrera-Ayala [1], Gerardo Tapia [2] and Juan Pedro Ferrio [1,3,*]

[1] Departamento de Botánica, Facultad de Ciencias Naturales y Oceanográficas, Universidad de Concepción, Concepción 4070386, Chile
[2] Unidad de Recursos Genéticos Vegetales, Instituto de Investigaciones Agropecuarias, INIA-Quilamapu, Chillán 3800062, Chile
[3] ARAID-Departamento de Sistemas Agrícolas, Forestales y Medio Ambiente, Centro de Investigación y Tecnología Agroalimentaria de Aragón (CITA), 50059 Zaragoza, Spain
* Correspondence: jpferrio@cita-aragon.es; Tel.: +34-976-716374

Abstract: Leaf hydraulic conductance (K_{Leaf}) is a measure of the efficiency of water transport through the leaf, which determines physiological parameters such as stomatal conductance, photosynthesis and transpiration rates. One key anatomical structure that supports K_{Leaf} is leaf venation, which could be subject to evolutionary pressure in dry environments. In this context, it is useful to assess these traits in species from arid climates such as *S. peruvianum* and *S. chilense*, in order to determine their hydraulic strategy and potential aptitude for the improvement of domestic tomato (*S. lycopersicum*). In this work, we measured K_{Leaf}, vein density, together with leaf water isotope composition ($\delta^{18}O$, $\delta^{2}H$) and leaf carbon isotope composition ($\delta^{13}C$), from which we derived proxies for outside-vein hydraulic resistance (R_{ox}) and intrinsic water use efficiency (WUE_i), respectively. The two wild species showed contrasting hydraulic strategies, with *S. chilense* performing as a water-spender, whereas *S. peruvianum* showed a water-saving strategy. Interestingly, *S. lycopersicum* was rather conservative, and showed the highest WUE_i. The low water transport capacity of *S. peruvianum* was not explained by vein density traits, but was related with the effective pathlength *L*, an isotope-derived proxy for R_{ox}. The low WUE_i of *S. peruvianum* suggest strong photosynthetic limitations. Our results show a wide diversity in water-use strategies in the genus, encouraging a detailed characterization of wild relatives. From a methodological point of view, we provide evidence supporting the use of water isotopes to assess changes in mesophyll hydraulic conductance, not attributable to vein density.

Keywords: leaf hydraulic conductance; vein density; stable isotopes; leaf water enrichment; effective pathlength *L*; carbon isotope discrimination; wild relatives; tomato; water use efficiency

Citation: Barrera-Ayala, D.; Tapia, G.; Ferrio, J.P. Leaf Carbon and Water Isotopes Correlate with Leaf Hydraulic Traits in Three *Solanum* Species (*S. peruvianum*, *S. lycopersicum* and *S. chilense*). *Agriculture* **2023**, *13*, 525. https://doi.org/10.3390/agriculture13030525

Academic Editors: Ivan Francisco Garcia Tejero and Victor Hugo Durán-Zuazo

Received: 13 January 2023
Revised: 13 February 2023
Accepted: 20 February 2023
Published: 22 February 2023

1. Introduction

Water availability is the most important factor limiting the photosynthesis and growth of plants, especially in arid and semi-arid zones [1,2]. The regulation of water use is often considered to be primarily dominated by interactions between xylem architecture and stomatal behavior [1,2] and this may covary to optimize water use [3,4]. In this regard, plants with a conservative strategy (water savers) would reduce water use, but at the expense of a limited carbon gain; conversely, water spenders can keep higher growth rates, but require a higher water transport capacity [1–3]. In this regard, leaves constitute the main bottleneck for whole-plant hydraulic capacity, accounting for ca. 30% of the whole-plant resistance to water movement, and leaf hydraulic conductance (K_{Leaf}) becomes a key limiting factor for water use and photosynthesis across a wide range of species [3–5].

The main water path through the leaves includes a complex system of serial and parallel xylem veins. In dicotyledons, venation consists of three major vein orders, and

up to five minor vein orders, and the hydraulic limitation of a given vein order depends inversely on its density (and redundancy), relative to the other vein orders [3,6]. Hence, a denser vein system, and a larger proportion of major veins, would allow higher water transport capacity, and thus higher K_{Leaf} [3,6]. In this sense, a higher major and minor vein density has been reported for drought-tolerant species, because this provides alternative pathways for water flow around embolized veins [7,8]. Alternatively, the proportion between major and minor vein density has been proposed as an indicator of hydraulic vulnerability [6]. However, the association between leaf venation and K_{leaf} across species is not always consistent and depends on the scale of the comparison [5,7,9].

Besides the xylem pathway, water also needs to move outside veins, through the bundle sheath and the mesophyll, and this pathway accounts for 30–80% of the total leaf hydraulic resistance to water flow [3,6,9]. So far, estimates of the xylem and outside-xylem components of K_{Leaf} (K_x and K_{ox}, respectively) have relied on either modeling approaches or tedious and invasive vein-cutting experiments [6,9]. In this context, the isotopic composition of leaf water has been proposed as an alternative approach to estimate K_{ox} [10–12]. Briefly, during transpiration, leaf water is enriched in the heavier isotopes ^{18}O and ^{2}H, and this can be modeled from environmental drivers such as leaf temperature and relative humidity [13–15]. However, actual enrichment of the whole leaf lamina is lower than modeled values for the sites of evaporation due to the mass flow of non-enriched water, driven by transpiration, causing the so-called *Péclet* effect [13,14]. The magnitude of this effect is proportional to the transpiration rate, and the effective pathlength (L, in m), which accounts for the length and tortuosity of the water pathway from the xylem to the evaporative surfaces [13,16]. Consequently, this parameter, determined empirically, can provide a non-manipulative proxy for the outside-vein hydraulic resistance (i.e., the inverse of K_{ox}). Up to now, this has been tested in a limited number of species, with contradictory results [11,12,17,18]; therefore, additional assays are needed to define the limitations of this approach.

The positive association between K_{leaf} and maximum stomatal conductance is generally explained by the need to adjust water supply to water demand [5,19]. In turn, the association with photosynthesis and productivity would be mainly a consequence of stomatal constraints [4,5], reinforced by a covariation between K_{ox} and mesophyll conductance for CO_2 [11,12,20,21]. Hence, the coordination of K_{Leaf} with photosynthesis generally implies a negative association between productivity and the ratio between photosynthesis and stomatal conductance (intrinsic water-use efficiency, WUE_i). However, the sign of this association depends on the leading term in the quotient, with two main scenarios, as defined in Fardusi et al. [22]. In the first scenario, higher WUE_i results from an increase in photosynthesis, independent from stomatal conductance, and we would expect a positive relationship with plant productivity [22,23]. In the second scenario, higher WUE_i is mainly driven by stomatal limitations, and we would expect a negative association with growth and photosynthesis [24,25]. Although the general trend between K_{leaf} and photosynthesis fits with the second scenario, it has been observed, for example, that tropical rainforest species (adapted to wet soils and low atmospheric water demand) show higher potential photosynthesis than temperate trees for a given K_{leaf} [19,26]. However, it is unclear how species adaptation to different combinations of soil dryness and atmospheric demand affects the coordinated response of K_{leaf} and WUE_i [3,18,27].

In summary, despite the existence of general trends across multiple species, the link between vein traits, K_{Leaf} and WUE_i is not straight-forward, differing across genera and species with distinct evolutionary history [4,7,8,18]. In this context, the tomato and its wild relatives constitute a model for the study of plants' adaptation to drought and other environmental constraints [28–31]; however, the water use strategy of tomato wild relatives has not yet been assessed from a leaf hydraulics perspective. The *Lycopersicon* clade comprises the domesticated tomato (*Solanum lycopersicum* L.) and 12 closely related species, with a broad geographic and ecological distribution along western South America, including deserts, tropical rainforests and highlands [29,32,33]. In this work, we focused on two wild relatives

(*Solanum peruvianum* L. and *Solanum chilense* Dunal) that can be found in arid and saline habitats (e.g., in the Atacama desert) but display different geographic and microhabitat preferences [29,30,32,33]. *S. peruvianum* has a wide distribution but is more common in the coastal areas of Perú, up to 2500 m.a.s.l., often in fog oases known as *lomas*, and occasionally growing as a weed in irrigated crops [29,30,32]. *S. chilense* is mainly found in northern Chile; it also appears in the *lomas*, but spreads to more continental areas and higher altitudes (up to 3500 m.a.s.l.), growing in dry river beds and ravines with stony soils, surviving in hyper-arid environments by deep roots [30,32,33]. To characterize the water use strategy of these two species, we combined measurements of leaf hydraulic conductance, leaf venation and the isotopic enrichment of leaf water, using a commercial tomato cultivar as a reference. We hypothesized that the wild relatives, more drought-adapted than the domesticated tomato, would show a conservative water-use strategy, associated with high minor vein density (high redundance), but low major vein density and leaf conductance. However, this tendency would be more exacerbated in *S. chilense*, which can thrive in drier areas. As a second aim, we assessed the association between WUE_i and physiological and anatomical traits related to water transport. In this regard, following the hypothesized conservative strategy, we anticipated a higher WUE_i in the two wild relatives than in the domesticated tomato. Finally, from a methodological point of view, we aimed to test the potential of the isotope-derived parameter *L* as a proxy for outside-vein hydraulic resistance, assessing its association with water-transport traits.

2. Materials and Methods

2.1. Plant Material

Seeds of *S. lycopersicum* (var. 'Moneymaker'), *S. peruvianum* (Acc. Q958) and *S. chilense* (Acc. Q966) were provided by Germplasm Bank Network of the Instituto de Investigaciones Agropecuarias (INIA) under a standard material transfer agreement and an Institutional INIA Policy for ABS of plant genetic material following international agreement signed by Chile (see Appendix A, Table A1 for details). The seeds were germinated in a growth chamber during one month, with photoperiod 18/6 h light-dark, at 25/18 °C and 60% relative humidity. Later, the plantlets were relocated to the greenhouse. Leaves were obtained from plants grown in greenhouse under optimal conditions at the end of October (*S. chilense* (SC), n = 5; *S. peruvianum* (SP), n = 10; *S. lycopersicum* (SL) n = 6). Collected leaves were stored at ambient temperature in glass flasks filled with distilled water and covered with black nylon until K_{Leaf} measure.

2.2. Leaf Hydraulics

Leaf hydraulic conductance was determined by the Evaporative Flux Method [5]. Prior to the measurement, the leaf was hydrated overnight, in dark conditions to avoid water loss by transpiration. Leaves were placed at the same height as the water reservoir to ensure that the water movement was driven by transpiration, instead of being forced by positive pressure due to gravity. Leaves were illuminated with 1000 µmol $m^{-2}s^{-1}$ PAR (module CI-301 LA, CID Bioscience Inc., Camas, OR, USA), maintaining a stable leaf temperature between 23 °C and 28 °C. Each leaf was connected for ca. 20 min to reach steady-state conditions. Then, the weight change of the water reservoir was recorded every 30 s during 15 min to determine water flow (*E*, in g s^{-1}, then converted to mmol s^{-1}). At the end of the protocol, the leaf was removed from the system and stored in a sealed plastic bag for 20 min to prevent water loss, and leaf water potential (Ψ_{Leaf}, in Mpa) was determined with a Scholander chamber. Total leaf hydraulic conductance (*K*) was first determined as the ratio between *E* and the water potential gradient from the water reservoir to the leaf ($\Psi_{source} - \Psi_{Leaf}$), assuming Ψ_{source} = 0 Mpa. Area-adjusted leaf hydraulic conductance (K_{Leaf}) was then calculated by dividing *K* by leaf area. Following [5], K_{Leaf} was normalized at a temperature of 20 °C to account for temperature-dependent changes in water viscosity. Finally, total leaf conductance to water vapor (g_w) was estimated from measured flow and the water vapor gradient from the intercellular space to ambient air, in molar fraction (w_i-

w_a, in mol H_2O mol air^{-1}). The molar fraction gradient was calculated from air temperature and relative humidity (monitored in situ during the experiment with a thermo-hygrometer), leaf temperature (measured with a calibrated K-type thermocouple) and mean atmospheric pressure of 99.5 kPa, based on data from a nearby agrometeorological station (Santa Rosa Experimental Station, INIA-Quilamapu, 36°32′ S; 71°54′ W; 195 m a.s.l.).

2.3. Leaf Water Distillation and Isotope Composition

After measuring K_{Leaf}, the midrib was removed for each leaflet and the leaf lamina stored in sealed glass vials and kept at −80 °C until cryogenic distillation. The leaf lamina water was extracted by cryogenic vacuum distillation, as described in Palacio et al. [34]. The samples (inside of glass vials) were submerged in a water bath at 80 °C to facilitate the evaporation of leaf lamina water and connected to the vacuum pressure distilling system at −760 in Hg (−0.88 MPa), where the water condenses in glass collector submerged in liquid N. Samples were stored in sealed glass vials at 4 °C until analysis. As a reference value for source water, we took two aliquots from the distilled water used to determine K_{Leaf}. Isotope composition of water ($\delta^{18}O$, $\delta^{2}H$) was determined by infra-red laser spectroscopy (CRDS) at the Serveis Científico-Tècnics of Universitat de Lleida (Lleida, Spain), using a water isotopes analyzer Picarro L2120-I (Picarro Inc., Sunnyvale, CA, USA), coupled to a high-precision vaporizer (A0211). The possible spectral interference caused by organic contaminants was corrected following [35].

2.4. Modeling Isotopic Enrichment of Leaf Water

Isotopic enrichment of leaf lamina relative to source water ($\Delta^{18}O$, $\Delta^{2}H$) was calculated from $\Delta_L = (\delta_L - \delta_S)/(1 + \delta_S)$, where δ_L and δ_S are the isotope composition ($\delta^{18}O$, $\delta^{2}H$) of leaf-lamina and source water, respectively. Isotopic enrichment at the sites of evaporation under steady state (Δ_e) were modeled using the Craig and Gordon model, as adapted to plant leaves by Dongman et al. [36].

$$\Delta_e = \varepsilon^+ + \varepsilon_k + (\Delta_v - \varepsilon_k)\,\frac{e_a}{e_i} \quad (1)$$

where ε^+ is the equilibrium fractionation between liquid water and vapor, ε_k is the kinetic fractionation of vapor diffusion from the leaf to the atmosphere, Δ_v is the isotopic enrichment of atmospheric water vapor and e_a/e_i is the ratio of ambient to intercellular vapor pressures. Fractionation factors were taken from the literature, as detailed elsewhere [10]. The steady-state isotopic enrichment of leaf lamina water (Δ_{Lss}) was calculated by correcting for the gradient from xylem water to enriched water at the sites of evaporation, the *Péclet* effect [13]:

$$\Delta_{Lss} = \Delta_e \frac{1 - e^{-\varphi}}{\varphi},\ \varphi = \frac{E \cdot L}{C \cdot D} \quad (2)$$

where φ is the *Péclet* number, E is the leaf transpiration rate, L is the scaled effective path length (m) for water movement from the veins to site of evaporation, C is the molar concentration of water (5.56 10^3 mol m^{-3}) and D is the tracer diffusivity (m^2 s^{-1}) of the heavy water isotopologue ($H_2{}^{18}O$/HDO) in 'light' water (H_2O), corrected by temperature, as described in [10]. The effective pathlength L under steady-state assumption (L_{ss}) was determined by fitting Equation (2) to the *Péclet* number:

$$L_{ss} = \frac{\varphi \cdot C \cdot D}{E} \quad (3)$$

2.5. Leaf Carbon Isotope Composition

Carbon isotope composition ($\delta\ ^{13}C$) was determined from leaf dry matter, as a proxy for WUE_i [13,22,37]. For that, the dry material remaining after water distillation was ground in mortar until obtaining a fine powder. Isotope ratios were determined using a combustion and gas preparation module (EA-GSL Elemental Analyzer, Sercon, UK) attached to an

Isotope Ratio Mass Spectrometer (20–22 IRMS, Sercon, UK) at the Soil, Water and Forest Lab (LISAB, Universidad de Concepción, Chile).

2.6. Leaf Vein Density

In each measured leaf, the terminal leaflet was cut for leaf vein density analysis. The leaflet was diaphanized according to Scoffoni et al. [8]. The leaflets were treated with NaOH at 5% for five days at ambient temperature. After this period, the samples were rinsed with distilled water to remove the NaOH, remaining in vacuum for 10 min. Then, the leaflets were bleached with sodium hypochlorite at 50% and washed with distilled water several times. Later, the leaflets were dehydrated in alcohol baths with ascending concentrations (30, 50, 70 and 95%), remaining five minutes in each bath, then placed in a safranin 1% bath for 24 h. Excess safranin was removed under vacuum and the samples were rehydrated following the series of alcohol baths in descending order. Finally, 2.5 × 2.5 cm bleached leaflet sections were mounted in distilled water for the quantification of leaf venation. Pictures were taken under two objective lenses (0.67× for major veins and 3× for minor veins), taking measures in three leaflet subsectors (from base to tip). ImageJ (1.5r version, National Institutes of Health, Bethesda, Maryland, USA) was used to measure major vein density (MVD) in the image and the result of MVD was divided by the image area (15.61 × 11.66 mm). Minor vein density (mVD) was measured in the same way in a smaller image area (3.39 × 2.53 mm). Finally, the data obtained in each subsector were averaged to obtain one datum per leaflet. TotalVD was calculated as the sum of MVD and mVD.

2.7. Statistical Analysis

Data were analyzed by ANOVA, previously checking for the assumption of normality and homoscedasticity. For variables following these assumptions, we performed a One-Way ANOVA and applied the multiple comparison test of LSD Fisher, due to heterogeneous sample size. Conversely, for non-normal and heteroscedastic variables we used the Kruskal–Wallis (K–W) test, and the multiple comparison test of Dunn. The assessment of possible relations between variables was performed using two correlation analyses, Pearson and Spearman, both with significance level of $p < 0.05$. Multivariate association of leaf hydraulics and isotopic variables was performed by a Principal Component Analysis (PCA), using zero mean. Statistical analysis was performed in SigmaPlot 11.0 and PCA was performed in RStudio (version 1.2.1335) with *vegan* package. The full dataset is available in Supplementary Materials Table S1.

3. Results

3.1. Leaf Vein Density

The leaf vein density traits of *S. lycopersicum*, *S. peruvianum* and *S. chilense* are summarized in Figure 1. The ANOVA showed significant differences in total vein density (TotalVD; $p = 0.025$). *S. lycopersicum* was the species with the highest TotalVD (6.81 mm mm^{-2}) followed by *S. peruvianum* (5.92 mm mm^{-2}) and *S. chilense* (5.53 mm mm^{-2}), although only *S. lycopersicum* and *S. chilense* differed significantly according to the Fisher test (Figure 1A). Major vein density (MVD) was significantly different between the species ($p = 0.014$), although only the extremes (*S. chilense* and *S. lycopersicum*) differed significantly (Figure 1B). Contrary to TotalVD, *S. chilense* showed the highest MVD (0.33 mm mm^{-2}), followed by *S. peruvianum* (0.28 mm mm^{-2}) and *S. lycopersicum* (0.26 mm mm^{-2}). Minor vein density (mVD) was significantly different among the three species ($p < 0.001$). *S. lycopersicum* showed the highest mVD (5.71 mm mm^{-2}), followed by *S. peruvianum* (4.94 mm mm^{-2}) and *S. chilense* (3.01 mm mm^{-2}) (Figure 1D). Finally, the K–W test showed significant differences in the ratio of major vein density to minor vein density (MVD/mVD; $p = 0.001$), with *S. chilense* (0.11) showing significantly higher median than *S. lycopersicum* and *S. peruvianum* (0.045 and 0.06, respectively; Figure 1C).

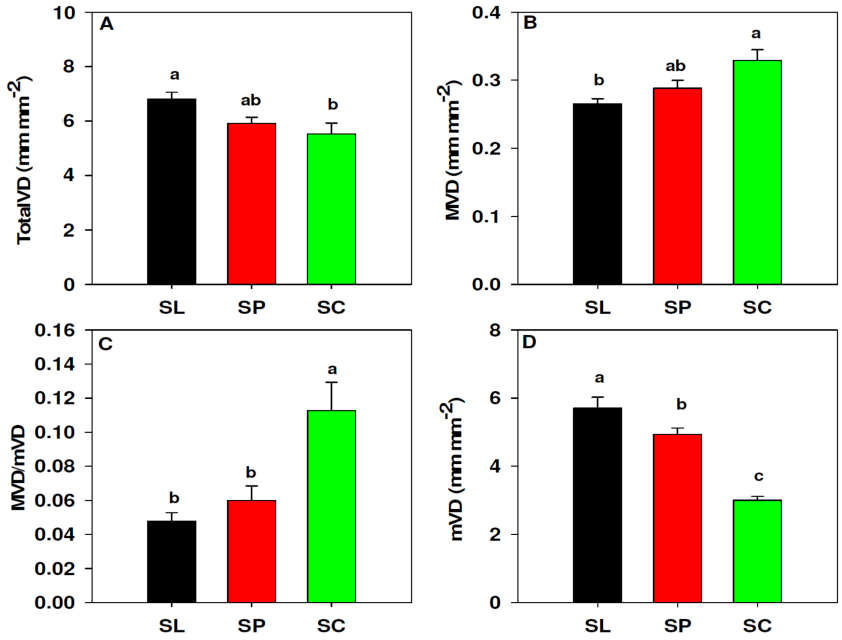

Figure 1. Differences in leaf venation between *S. lycopersicum* (black, SL), *S. peruvianum* (red, SP) and *S. chilense* (green, SC). Total vein density, TotalVD (**A**), major vein density, MVD (**B**), ratio of MVD to mVD, MVD/mVD (**C**), minor vein density, mVD (**D**). Values in (**A**,**B**,**D**) represent the mean and the error bars represent standard error. Values in (**C**) represent the median analyzed by Kruskal–Wallis analysis and error bars represent the 75% percentile. Different letters indicate significant differences ($p < 0.05$) according to Fisher (**A**,**B**,**D**) and Dunn's (**C**) tests.

3.2. Leaf Hydraulic Conductance

Leaf hydraulic traits are summarized in Figure 2. We found significant differences in water flux (E; $p = 0.005$), with *S. chilense* showing significantly higher median (4.58 mmol m^{-2} s^{-1}) than *S. peruvianum* (0.70 mmol m^{-2} s^{-1}, respectively) (Figure 2A). *S. lycopersicum* (2.22 mmol m^{-2} s^{-1}) was not statistically different from the other two species. The three species differed significantly in leaf water potential (Ψ_{Leaf}; $p < 0.001$). *S. chilense* showed significantly less negative Ψ_{Leaf} (−0.24 MPa) than *S. lycopersicum* and *S. peruvianum* (−0.47 and −0.59 MPa, respectively) (Figure 2B). Area-adjusted leaf hydraulic conductance (K_{Leaf}) showed significant differences between species ($p < 0.001$). *S. chilense* had a higher median K_{Leaf} (18.42 mmol m^{-2} s^{-1} MPa^{-1}) than *S. peruvianum* (1.24 mmol m^{-2} s^{-1} MPa^{-1}), whereas *S. lycopersicum* (4.43 mmol m^{-2} s^{-1} MPa^{-1}) was not statistically different from both species (Figure 2C). Total leaf hydraulic conductance (K) also showed significant differences between species ($p = 0.002$). Similar to K_{Leaf}, *S. chilense* had a higher median for K (0.046 mmol s^{-1} MPa^{-1}) than *S. peruvianum* (0.00655 mmol s^{-1} Mpa^{-1}), while *S. lycopersicum* (0.0183 mmol s^{-1} Mpa^{-1}) was not statistically different from both species (Figure 2D).

3.3. Leaf Water Isotopic Enrichment

The isotopic enrichment of leaf water and related variables are summarised in Figure 3. The three species differed significantly in $\Delta^{18}O$ ($p < 0.001$) and $\Delta^{2}H$ ($p = 0.003$). *S. lycopersicum* showed significantly higher $\Delta^{18}O$ and $\Delta^{2}H$ (11.4‰ and 42.7‰, respectively; Figure 3A,B) than *S. peruvianum* (6.9‰; 30.6‰) and *S. chilense* (6.5‰; 25.8‰). *S. peruvianum* and *S. chilense*, however, were not significantly different. Effective path length (L_{ss}), either calculated from ^{18}O or ^{2}H (Figure 3C,D), showed significant differences among species ($p = 0.009$ and $p = 0.003$, for $L_{ss}{}^{18}O$ and $L_{ss}{}^{2}H$, respectively). *S. peruvianum* showed significantly higher L_{ss} (301.7 mm, averaging ^{18}O and ^{2}H estimates) than *S. lycopersicum* (27.50 mm) and *S. chilense* (48.5 mm). The L_{ss} of *S. lycopersicum* and *S. chilense* did not differ significantly.

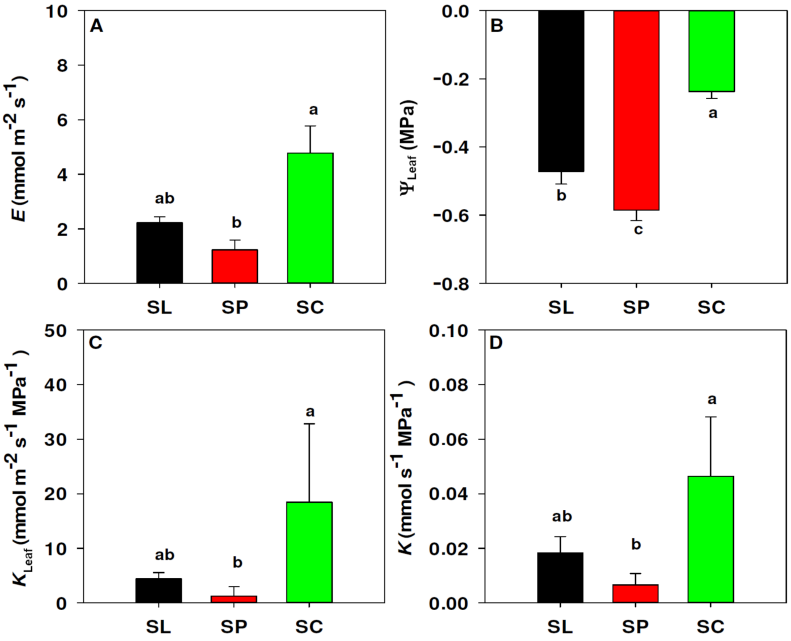

Figure 2. Differences in leaf hydraulics between *S. lycopersicum* (black, SL), *S. peruvianum* (red, SP) and *S. chilense* (green, SC). Water flux *E* (**A**), water potential Ψ_{Leaf} (**B**), area-adjusted leaf hydraulic conductance K_{Leaf} (**C**) and total leaf hydraulic conductance *K* (**D**). Values in (**A**,**C**,**D**) represent the median and 75% percentile. Values in (**B**) represent the mean and standard error. Different letters represent significant differences ($p < 0.05$) according to Fisher (**B**) and Dunn's (**A**,**C**,**D**) tests.

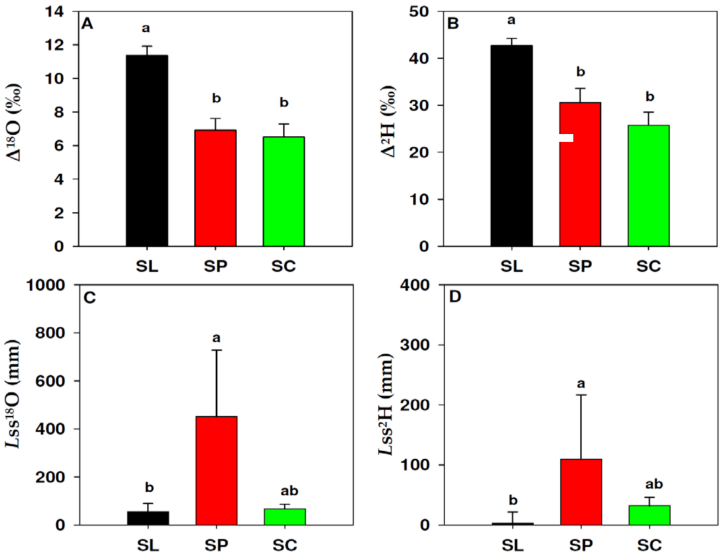

Figure 3. Leaf water enrichment traits in *S. lycopersicum* (black, SL), *S. peruvianum* (red, SP) and *S. chilense* (green, SC). $\Delta^{18}O$ and $\Delta^{2}H$, oxygen (**A**) and hydrogen (**B**) leaf water isotopic enrichment; $L_{ss}{}^{18}O$ and $L_{ss}{}^{2}H$, effective path length, calculated from $\Delta^{18}O$ and $\Delta^{2}H$. Values in (**A**,**B**) represent the mean and standard error. Values in (**C**,**D**) represent the median and 75% percentile. Letters indicate significant differences ($p < 0.05$) according to Fisher (**A**,**B**) and Dunn's (**C**,**D**) tests.

3.4. Leaf Conductance to Water Vapour and $\delta^{13}C$

Leaf conductance to water vapour (g_w) showed significant differences between species ($p = 0.005$). The g_w of *S. chilense* (247.90 mmol m^2 s^{-1}) was higher than *S. peruvianum* (32.01 mmol m^2 s^{-1}), whereas *S. lycopersicum* (131.54 mmol m^2 s^{-1}) was not significantly different from the other two species (Figure 4A). Carbon isotope composition ($\delta^{13}C$) also differed significantly between species ($p < 0.001$): *S. lycopersicum* (−28.34‰) was less

negative than *S. peruvianum* and *S. chilense* (−29.69 and −30.13 ‰, respectively) (Figure 4B).

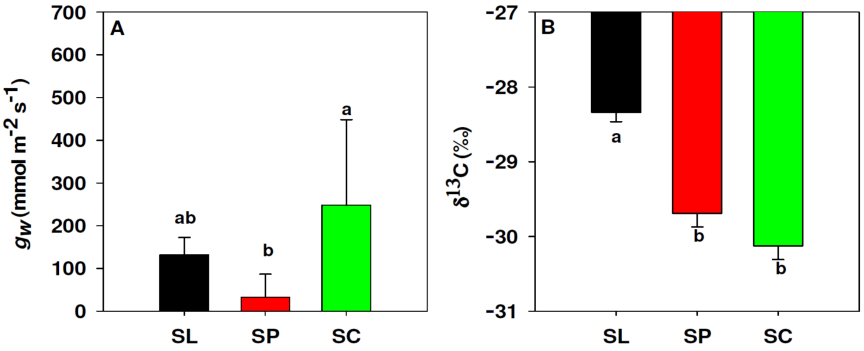

Figure 4. Differences in leaf conductance to water vapour, gw (**A**) and leaf isotope composition of ^{13}C, δ^{13}C (**B**) between *S. lycopersicum* (black, SL), *S. peruvianum* (red, SP) and *S. chilense* (green, SC). Values in (**A**) represent the median and 75% percentile. Values in (**B**) represent the mean and standard error. Letters indicate significant differences ($p < 0.05$) according to Fisher (**B**) and Dunn's (**A**) tests.

3.5. Correlation Analysis

The results of Pearson (*rp*, upper triangle) and Spearman (*rs*, lower triangle) correlation analysis among the most relevant variables are summarized in Table 1. Correlation analysis showed that leaf venation had a strong influence on leaf hydraulic variables. Interestingly, mVD was negatively correlated with K_{Leaf} ($rp = -0.67$, $p < 0.001$) and positively correlated with $\Delta^{18}O$ ($rp = 0.73$, $p < 0.01$), $\Delta^{2}H$ ($rp = 0.78$, $rs = 0.78$, $p < 0.001$) and $\delta^{13}C$ ($rp = 0.67$, $p < 0.01$). Major vein density showed generally weaker correlations than mVD, and the opposed sign, i.e., positive with K_{Leaf} ($rp = 0.49$, $p < 0.05$), and negative with $\Delta^{18}O$, $\Delta^{2}H$, L_{ss} and $\delta^{13}C$ (*rs* between −0.57 and −0.51, $p < 0.05$). The ratio between MVD and mVD, MVD/mVD, was also positively associated with K_{Leaf} ($rp = 0.77$, $p < 0.001$). However, MVD/mVD was negatively correlated with $\Delta^{18}O$, $\Delta^{2}H$ and $\delta^{13}C$, although these correlations showed a better adjustment with the Spearman rank correlation (*rs* between −0.71 and −0.76, $p < 0.01$). TotalVD was positively related to $\Delta^{18}O$ ($rp = 0.72$, $p < 0.001$), $\Delta^{2}H$ ($rp = 0.74$, $p < 0.001$) and $\delta^{13}C$ ($rp = 0.66$, $p < 0.01$). On the other hand, L_{ss} was negatively associated with K_{Leaf} ($rs = -0.61$, $p < 0.05$) and $\Delta^{18}O$ ($rs = -0.53$, $p < 0.01$) and positively correlated with MVD (rs = 0.51, $p < 0.05$).

Table 1. Correlation analysis of leaf hydraulics, isotopes and venation traits in the three species here studied. Upper triangle corresponds to result of Pearson correlation; lower triangle corresponds to Spearman correlation. K_{Leaf}, area-adjusted leaf hydraulic conductance (mmol m^{-2} s^{-1} MPa^{-1}); $\Delta^{18}O$ and $\Delta^{2}H$, oxygen and hydrogen isotopic enrichment of leaf water (‰); L_{ss}, mean effective path length (mm); $\delta^{13}C$, carbon isotope composition (‰); TotalVD, MVD and mVD, total, major and minor vein density (mm mm^{-2}).

9	K_{Leaf}	$\Delta^{18}O$	$\Delta^{2}H$	L_{ss}	$\delta^{13}C$	TotalVD	MVD	mVD	MVD/mVD
K_{Leaf}		−0.47	−0.59 *	−0.43	−0.40	−0.3	0.49 *	−0.67 ***	0.77 ***
$\Delta^{18}O$	−0.13		0.97 ***	−0.29	0.78 **	0.72 **	−0.55 *	0.73 **	−0.66 **
$\Delta^{2}H$	−0.34	0.94 ***		−0.16	0.78 **	0.74 **	−0.49	0.78 ***	0.72 **
L_{ss}	−0.61 *	−0.53 *	−0.36		−0.20	−0.18	0.21	0.06	−0.10
$\delta^{13}C$	−0.21	0.68 **	0.68 **	−0.42		0.66 **	−0.464	0.67 **	−0.58 *
TotalVD	−0.17	0.54 *	0.62 *	−0.25	0.61 *		−0.173	0.69 ***	−0.45 *
MVD	0.18	−0.57 *	−0.51 *	0.51 *	−0.51 *	−0.24		−0.54 *	0.78 ***
mVD	−0.48 *	0.63 *	0.78 ***	−0.06	0.63 *	0.70 ***	−0.54 *		−0.91 ***
MVD/mVD	0.42	−0.71 **	−0.76 ***	0.29	−0.72 **	−0.59 **	0.83 ***	−0.83 ***	

*** $p < 0.001$; ** $p < 0.01$; * $p < 0.05$.

3.6. Principal Component Analysis

To assess the association between variables, we performed a PCA with the most relevant variables (Figure 5A). The first two components of the PCA explained *ca*. 76% of the variability in leaf traits. The first axis (PC1) captured most of the variability associated with leaf hydraulic traits across the three species studied, explaining 56% of the total variation. The first axis (PC1) showed particularly strong loadings for mVD, MVD/mVD and K_{Leaf}. The second axis (PC2) explained ca. 20% of the total variation, and only showed a strong loading for L_{ss}. In general, a tight association between variables was observed (i.e., narrow angle between vectors), which was consistent with the correlation analysis (Table 1). Traits linked to higher water transport capacity were positively correlated with PC1 (e.g., MVD, MVD/mVD and K_{Leaf}), whereas traits associated with lower water transport capacity (e.g., mVD) were negatively correlated. All the traits included in the PCA had a strong influence, and clearly differentiated the species in three groups, representative of contrasting hydraulic strategies (Figure 5B). *S. lycopersicum* and *S. chilense* fell on opposite sides of PC1. *S. lycopersicum* showed higher values of mVD, $\delta^{13}C$, TotalVD and $\Delta^{18}O$, which is consistent with a conservative hydraulic strategy. Conversely, *S. chilense* showed higher values of MVD/mVD, K_{Leaf}, Ψ_{Leaf} and MVD, indicative of a water-spender hydraulic strategy. On the other hand, *S. peruvianum* had intermediate scores along PC1, but was clearly discriminated by PC2, being mainly associated with high values of L_{ss}, and, to a lesser extent, low values of Ψ_{Leaf}, $\Delta^{18}O$, $\delta^{13}C$ and K_{Leaf}.

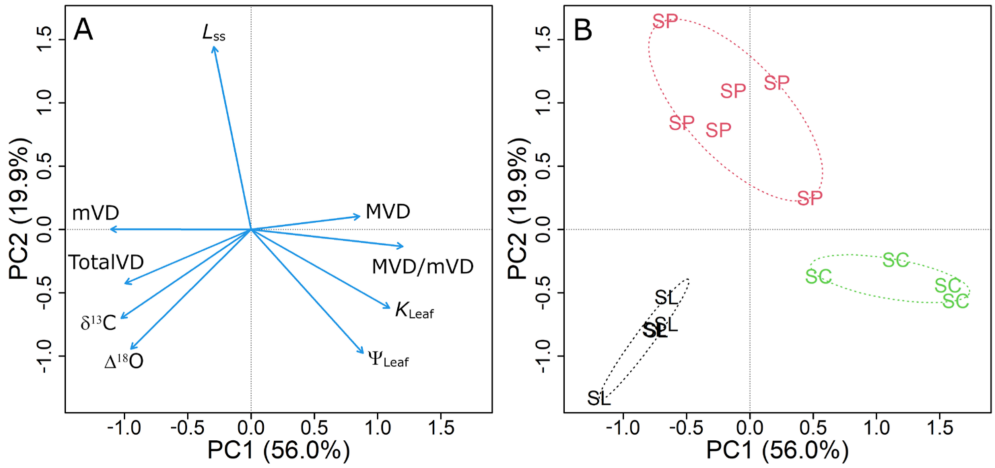

Figure 5. Principal component analysis (PCA) for leaf hydraulics, isotopes and venation variables among the three species here studied. The variable loading plot (**A**) shows the variables as blue arrows: Ψ_{Leaf}, leaf water potential; K_{Leaf}, leaf hydraulic conductance; MVD, mVD and MVD/mVD, major, minor vein density and major/minor vein ratio; L_{ss}, mean effective path length; $\delta^{13}C$, leaf carbon isotope composition; $\Delta^{18}O$, isotopic enrichment of leaf water. The scores plot (**B**) shows the score of each replicate along the PCA axis, indicating the species grouping: *S. lycopersicum* (SL), *S. peruvianum* (SP) and *S. chilense* (SC) and their respective ellipsoid hulls.

4. Discussion

4.1. Contrasting Hydraulic Strategies in Tomato Wild Relatives

The three tomato species assessed showed contrasting water transport capacities, which were partly explained by differences in leaf venation, in agreement with previous studies [3,5,7,8]. To the best of our knowledge, wild tomato species have not been characterized under a hydraulic approach, but their TotalVD and K_{Leaf} fell in the range of other herbaceous plants [7,8,20]. Nevertheless, K_{Leaf} showed a wide range across species, from *S. peruvianum*, in the lowest range for Angiosperms, to the upper-intermediate values of *S. lycopersicum* and *S. chilense* [3,5,12,20]. Across the three species, K_{Leaf} was best explained by the ratio between MVD and mVD, supporting the postulated functions of major and minor veins as main water suppliers and modulators of the extra-xylematic pathways,

respectively [6,9]. Contrary to our first hypothesis, we found that *S. chilense* had the highest MVD, but the lowest mVD, which resulted in a high K_{Leaf}. This reveals a water-spender strategy for this species, contrasting with the rather conservative responses of *S. lycopersicum* and *S. peruvianum*. In this regard, the microhabitat preferences of *S. chilense*, which is found in rocky soils and ravines, indicates that this species relies on a highly effective water uptake, taking advantage of deep or interstitial water reservoirs, as previously reported for other deep-rooted semiarid species [32,34]. Conversely, *S. peruvianum* showed intermediate vein densities, but the lowest K_{Leaf}. Anatomical traits could explain the contrasting water transport capacity of *S. lycopersicum* and *S. chilense* but did not explain the lower K_{Leaf} of *S. peruvianum*, pointing towards large extra-xylematic limitations to water flow in this species [9,20]. This is further supported by the high L_{ss} values (in the upper range of herbaceous species [11,12,18]), indicative of a particularly tortuous water pathway from the xylem to the sites of evaporation, i.e., lower K_{ox} [11,12,16,21]. This decline in K_{Leaf} due to low K_{ox} cannot be solely attributed to a smaller mVD (intermediate between *S. lycopersicum* and *S. chilense*), pointing towards functional differences in the mesophyll and/or bundle sheath [20]. Overall, the striking differences between *S. peruvianum* and *S. chilense* evidence that the two species have distinct ecological niches, despite a partially overlapping distribution. The strong hydraulic limitations of *S. peruvianum* suggest that this species is mainly adapted to dry environments, but with relatively low evaporative demand, such as the fog oases in coastal Peru [29,32]. Conversely, the adaptation of *S. chilense* to more continental habitats, with higher insolation and VPD, would require a higher water transport capacity to prevent leaf dehydration [3,26,27]. According to Tapia et al. [30], *S. chilense* also exhibits a stronger osmotic adjustment and proline accumulation than *S. peruvianum*, which would contribute to the maintenance of leaf turgor. In our study, the two species also differed in g_w, with higher values in *S. chilense* than in *S. peruvianum*, in agreement with the proposed coordination between K_{leaf} and gas exchange [5,19]. Our values are in range with those previously reported for *S. peruvianum* [4] (40–70 mmol m^{-2} s^{-1}) and other tomato cultivars [27,30] (60–100 mmol m^{-2} s^{-1}), whereas for *S. chilense* we found higher g_w than in Tapia et al. [30] (60–80 mmol m^{-2} s^{-1}). It should be noted that our approach to estimating g_w might be biased due to the assumption of steady-state water flow, which may not be the case if partial dehydration occurs (i.e., transpiration exceeding water inflow). However, this would cause an underestimation of g_w, rather than an overestimation, and mainly in species showing a significant drop in leaf water potential, such as *S. peruvianum*. Most likely, the generally higher g_w in our study would be due to the more limiting light conditions in previous works (150–300 µmol m^{-2} s^{-1} [27,30]; 1000 µmol m^{-2} s^{-1} in our case), particularly for *S. chilense*, the species most adapted to high radiation. Interestingly, *S. lycopersicum* showed an intermediate water use pattern, being closer to the conservative strategy of *S. peruvianum*. Although the results from a single cultivar (var. 'Moneymaker') cannot be extrapolated to the wide diversity of domesticated tomatoes, our values of vein density, K_{leaf} and g_w are similar to those reported by Du et al. [27] for the cultivars 'Jinpeng' and 'Zhongza', and also agree with the g_w reported by Tapia et al. [30] for cherry tomatoes (var. 'cerasiforme'), considered the ancestral form of domesticated tomato [32]. Besides the role of artificial selection, the similarities between *S. lycopersicum* and *S. peruvianum* may reflect the comparable habitat preferences of tomato ancestors [29,32].

4.2. Implications of Hydraulic Constraints for Water Use Efficiency

The PCA analysis further evidenced that the hydraulic strategy of *S. peruvianum* was more conservative than the other two species, but without a significant gain in WUE_i, as estimated from $\delta^{13}C$. Indeed, despite their contrasting water use patterns, *S. peruvianum* and *S. chilense* displayed similar values for $\delta^{13}C$, and both were more negative than *S. lycopersicum* (i.e., less WUE_i). Comparing *S. peruvianum* with *S. lycopersicum*, the lower $\delta^{13}C$ values were not linked to a higher g_w (scenario 2 in [22]) but would be explained by a lower photosynthetic capacity. In this regard, it has been reported in a wide range of tomato wild relatives that variation in mesophyll conductance to CO_2 (g_m) strongly affects

photosynthesis, with mesophyll limitations exceeding stomatal limitations [31]. Conversely, the low $\delta^{13}C$ of *S. chilense*, associated with high K_{Leaf} and g_w, would be consistent with a productive, water-spender strategy [scenario 1 in [22]). At this point, it has been argued that the leaf diffusion of CO_2 and H_2O share some common pathways, and hence K_{Leaf} and g_m are correlated, but this is still a matter of debate [11,12,20,21,38]. Although the K_{Leaf} of *S. peruvianum* was not statistically lower than *S. lycopersicum*, it was more limited hydraulically, according to the higher L_{ss}, and slightly lower mVD. Besides a direct relationship between K_{Leaf} and g_m, Ferrio et al. [11] also reported a negative association between L_{ss} and g_m in grapevine, further suggesting that mesophyll limitations may be responsible for the low $\delta^{13}C$ observed in *S. peruvianum*. Notably, MVD and mVD were inversely correlated across species, evidencing a tradeoff between water transport (high MVD and MVD/mVD), and reducing mesophyll limitations to gas exchange (high mVD), contradicting the general trends described by Brodribb et al. [5]. Again, this suggests that, for this particular set of species, water transport capacity and WUE_i responded independently to selective pressures. Most likely, this involves different combinations of mesophyll and stomatal limitations [31], which encourages further research on the links between g_m and K_{Leaf} across tomato wild relatives.

4.3. Potential and Limitations of Water Isotopes as Indicators of Hydraulic Constraints

Although the observed trends in K_{Leaf} and L_{ss} partly agree with our hypothesis (e.g., in the case of *S. peruvianum*), our results confirm that this association is not as straightforward as originally proposed. Other studies did not find a clear association between L_{ss} and K_{Leaf} [39], or even discuss the existence of a causal association between them, attributing it to methodological limitations and modeling assumptions [17,40]. One of these limitations is that evaporative gradients within the leaf may not be restricted to the mesophyll [41]. To solve this issue, the Farquhar–Gan model [41] considered not only a *Péclet* effect in the mesophyll, but also radial and longitudinal *Péclet* effects within the xylem network, which cause a progressive enrichment of leaf water from the midvein to the leaf margin. According to this model, major veins act as a sink of enriched water from minor veins, and these in turn act as a sink of enriched water from the mesophyll. Under the assumption that the *Péclet* effect is different for each leaf tissue (major and minor veins, mesophyll), L_{ss} could be related to anatomical traits such as vein density, just because leaf vein fraction influences the *Péclet* effect and thus the overall isotopic enrichment in leaf water [21,40]. However, it should be noted that in our study L_{ss} showed only a weak negative correlation with MVD, contrary to what would be expected if L_{ss} variations were driven by the fraction of water in leaf veins, as described in [40]. In particular, the high L_{ss} values in *S. peruvianum* could not be explained by the (intermediate) values in vein density. Furthermore, within this species, L_{ss} was negatively correlated with K_{Leaf} ($rs = -0.94$, $p = 0.017$), whereas vein traits were not significantly correlated with L_{ss} and K_{Leaf} ($p = 0.136$–1.000). Hence, despite the above-mentioned limitations, our study suggests that L_{ss} may still reflect differences in extra-xylematic water pathways, beyond anatomical effects. In this regard, this association deserves further exploration in a broad range of species and environments, e.g., taking advantage of recent advances in isotope laser spectroscopy, which allow non-destructive, continuous measurements of isotope fractionations within the leaves [21].

5. Conclusions

We confirmed our first hypothesis (more conservative water use in wild relatives) only for *S. peruvianum*, which shows a clear water-saving strategy, whereas *S. chilense* performs as a typical water spender. Although both species can grow in dry habitats, these strategies reflect adaptations to different levels of atmospheric water demand. Interestingly, vein density cannot explain the low K_{Leaf} of *S. peruvianum*, which is mostly attributable to high resistances in mesophyll water pathways, as suggested by the high L_{ss}. Our second hypothesis (higher WUE_i in wild relatives) was rejected, and indeed the domesticated tomato showed the highest WUE_i. In the case of *S. chilense*, the low WUE_i is consistent with

high stomatal conductances and a water-spender strategy. Conversely, the low WUE_i in the water-saving *S. peruvianum* points towards the mesophyll limitations of photosynthesis, indirectly evidenced through the unexpectedly low $\delta^{13}C$ and the large effective pathlength L_{ss}. From a methodological point of view, we support the use of L_{ss} to assess changes in the mesophyll components of K_{Leaf}, independent from vein density, as was the case for *S. peruvianum*.

Supplementary Materials: The following supporting information can be downloaded at: https://www.mdpi.com/article/10.3390/agriculture13030525/s1, Supplementary Table S1.

Author Contributions: Conceptualization, D.B.-A. and J.P.F.; methodology, D.B.-A. and J.P.F.; formal analysis, D.B.-A. and J.P.F.; resources, G.T. and J.P.F.; writing—original draft preparation, D.B.-A.; writing—review and editing, J.P.F. and G.T.; funding acquisition, J.P.F. All authors have read and agreed to the published version of the manuscript.

Funding: J.P.F. was supported by VRID-216.111.062-1 (Universidad de Concepción, Chile) and Grupo de Referencia H09_20R (Gobierno de Aragón, Spain).

Institutional Review Board Statement: Not applicable.

Data Availability Statement: The data presented in this study are available in the Supplementary Materials.

Acknowledgments: We thank Felipe Aburto and Alejandro Atenas (Laboratorio de Investigación en Suelos, Aguas y Bosques, Univ. Concepción) and Pilar Sopeña (Laboratorio de Silvicultura, Universitat de Lleida) for their assistance with isotope analysis. We thank Marcela Rodriguez and Roberto A. Rodríguez Ríos (Univ. Concepción) for the use of binocular microscopes and for providing materials for staining, respectively.

Conflicts of Interest: The authors declare no conflict of interest.

Appendix A

Table A1. Passport information from wild tomato accession.

Accession Number	Taxon	Latitude	Longitude	Elevation (m.a.s.l)	Location-Country
Q958	*S. peruvianum*	18°14′31.9″	70°9′8.7″	355	Tarapaca, Chile
Q966	*S. chilense*	18°16′52.7″	69°18′50.4″	3290	Tarapaca, Chile

References

1. McDowell, N.; Pockman, W.T.; Allen, C.D.; Breshears, D.D.; Cobb, N.; Kolb, T.; Plaut, J.; Sperry, J.; West, A.; Williams, D.G. Mechanisms of plant survival and mortality during drought: Why do some plants survive while others succumb to drought? *New Phytol.* **2008**, *178*, 719–739. [CrossRef] [PubMed]
2. Skelton, R.P.; West, A.G.; Dawson, T.E. Predicting plant vulnerability to drought in biodiverse regions using functional traits. *Proc. Nat. Acad. Sci. USA* **2015**, *112*, 5744–5749. [CrossRef] [PubMed]
3. Sack, L.; Holbrook, N.M. Leaf hydraulics. *Annu. Rev. Plant Biol.* **2006**, *57*, 361–381. [CrossRef] [PubMed]
4. Scoffoni, C.; Chatelet, D.S.; Pasquet-kok, J.; Rawls, M.; Donoghue, M.J.; Edwards, E.J.; Sack, L. Hydraulic basis for the evolution of photosynthetic productivity. *Nat. Plants* **2016**, *2*, 16072. [CrossRef]
5. Brodribb, T.J.; Field, T.S.; Jordan, G.J. Leaf maximum photosynthetic rate and venation are linked by hydraulics. *Plant Physiol.* **2007**, *144*, 1890–1898. [CrossRef]
6. McKown, A.D.; Cochard, H.; Sack, L. Decoding leaf hydraulics with a spatially explicit model: Principles of venation architecture and implications for its evolution. *Am. Nat.* **2010**, *175*, 447–460. [CrossRef]
7. Sack, L.; Scoffoni, C. Leaf venation: Structure, function, development, evolution, ecology and applications in the past, present and future. *New Phytol.* **2013**, *198*, 983–1000. [CrossRef]
8. Scoffoni, C.; Rawls, M.; McKown, A.; Cochard, H.; Sack, L. Decline of leaf hydraulic conductance with dehydration: Relationship to leaf size and venation architecture. *Plant Physiol.* **2011**, *156*, 832–843. [CrossRef]
9. Cochard, H.; Nardini, A.; Coll, L. Hydraulic architecture of leaf blades: Where is the main resistance? *Plant Cell Environ.* **2004**, *27*, 1257–1267. [CrossRef]

10. Ferrio, J.P.; Cuntz, M.; Offermann, C.; Siegwolf, R.; Saurer, M.; Gessler, A. Effect of water availability on leaf water isotopic enrichment in beech seedlings shows limitations of current fractionation models. *Plant Cell Environ.* **2009**, *32*, 1285–1296. [CrossRef]
11. Ferrio, J.P.; Pou, A.; Florez-Sarasa, I.; Gessler, A.; Kodama, N.; Flexas, J.; Ribas-Carbó, M. The Péclet effect on leaf water enrichment correlates with leaf hydraulic conductance and mesophyll conductance for CO_2. *Plant Cell Environ.* **2012**, *35*, 611–625. [CrossRef]
12. Flexas, J.; Barbour, M.M.; Brendel, O.; Cabrera, H.M.; Carriquí, M.; Díaz-Espejo, A.; Douthe, C.; Dreyer, E.; Ferrio, J.P.; Gago, J.; et al. Mesophyll diffusion conductance to CO_2: An unappreciated central player in photosynthesis. *Plant Sci.* **2012**, *193–194*, 70–84. [CrossRef]
13. Farquhar, G.D.; Lloyd, J. Carbon and oxygen isotope effects in the exchange of carbon dioxide between terrestrial plants and the atmosphere. In *Stable Isotopes and Plant Carbon-Water Relations*; Ehleringer, J.R., Hall, A.E., Farquhar, G.D., Eds.; Academic Press, Inc.: San Diego, CA, USA, 1993; pp. 47–70. [CrossRef]
14. Barbour, M.M.; Farquhar, G.D. Do pathways of water movement and leaf anatomical dimensions allow development of gradients in H218O between veins and the sites of evaporation within leaves? *Plant Cell Environ.* **2004**, *27*, 107–121. [CrossRef]
15. Cernusak, L.A.; Barbeta, A.; Bush, R.T.; Eichstaedt, R.; Ferrio, J.P.; Flanagan, L.B.; Gessler, A.; Martín-Gómez, P.; Hirl, R.T.; Kahmen, A.; et al. Do 2H and 18O in leaf water reflect environmental drivers differently? *New Phytol.* **2022**, *235*, 41–51. [CrossRef]
16. Cuntz, M.; Ogée, J.; Farquhar, G.D.; Peylin, P.; Cernusak, L.A. Modelling advection and diffusion of water isotopologues in leaves. *Plant Cell Environ.* **2007**, *30*, 892–909. [CrossRef]
17. Loucos, K.E.; Simonin, K.A.; Song, X.; Barbour, M.M. Observed relationships between leaf $H_2{}^{18}O$ Péclet effective length and leaf hydraulic conductance reflect assumptions in Craig-Gordon model calculations. *Tree Physiol.* **2015**, *35*, 16–26. [CrossRef]
18. Hommel, R.; Siegwolf, R.; Saurer, M.; Farquhar, G.D.; Kayler, Z.; Ferrio, J.P.; Gessler, A. Drought response of mesophyll conductance in forest understory species–impacts on water-use efficiency and interactions with leaf water movement. *Physiol. Plant.* **2014**, *152*, 98–114. [CrossRef]
19. Sack, L.; Cowan, P.D.; Jaikumar, N.; Holbrook, N.M. The 'hydrology' of leaves: Co-ordination of structure and function in temperate woody species. *Plant Cell Environ.* **2003**, *26*, 1343–1356. [CrossRef]
20. Flexas, J.; Scoffoni, C.; Gago, J.; Sack, L. Leaf mesophyll conductance and leaf hydraulic conductance: An introduction to their measurement and coordination. *J. Exp. Bot.* **2013**, *64*, 3965–3981. [CrossRef]
21. Barbour, M.M. Understanding regulation of leaf internal carbon and water transport using online stable isotope techniques. *New Phytol.* **2017**, *213*, 83–88. [CrossRef]
22. Fardusi, M.J.; Ferrio, J.P.; Comas, C.; Voltas, J.; Resco de Dios, V.; Serrano, L. Intra-specific association between carbon isotope composition and productivity in woody plants: A meta-analysis. *Plant Sci.* **2016**, *251*, 110–118. [CrossRef] [PubMed]
23. Gyenge, J.; Fernández, M.E.; Sarasola, M.; Schlichter, T. Testing a hypothesis of the relationship between productivity and water use efficiency in Patagonian forests with native and exotic species. *For. Ecol. Manag.* **2008**, *255*, 3281–3287. [CrossRef]
24. Araus, J.L.; Villegas, D.; Aparicio, N.; Del Moral, L.; El Hani, S.G.; Rharrabti, Y.; Ferrio, J.P.; Royo, C. Environmental factors determining carbon isotope discrimination and yield in durum wheat under Mediterranean conditions. *Crop Sci.* **2003**, *43*, 170–180. [CrossRef]
25. Voltas, J.; Chambel, M.R.; Prada, M.A.; Ferrio, J.P. Climate-related variability in carbon and oxygen stable isotopes among populations of Aleppo pine grown in common-garden tests. *Trees* **2008**, *22*, 759–769. [CrossRef]
26. Sack, L.; Tyree, M.T.; Holbrook, N.M. Leaf hydraulic architecture correlates with regeneration irradiance in tropical rainforest trees. *New Phytol.* **2005**, *167*, 403–413. [CrossRef]
27. Du, Q.; Jiao, X.; Song, X.; Zhang, J.; Bai, P.; Ding, J.; Li, J. The response of water dynamics to long-term high vapor pressure deficit is mediated by anatomical adaptations in plants. *Front. Plant Sci.* **2020**, *11*, 758. [CrossRef]
28. Moyle, L.C.; Muir, C.D. Reciprocal insights into adaptation from agricultural and evolutionary studies in tomato. *Evol. Appl.* **2010**, *3*, 409–421. [CrossRef]
29. Bauchet, G.; Causse, M. Genetic diversity in Tomato (*Solanum lycopersicum*) and its wild relatives. In *Genetic Diversity in Plants*; InTech: London, UK, 2012; pp. 161–162. [CrossRef]
30. Tapia, G.; Méndez, J.; Inostroza, L. Different combinations of morpho-physiological traits are responsible for tolerance to drought in wild tomatoes *Solanum chilense* and *Solanum peruvianum*. *Plant Biol.* **2016**, *18*, 406–416. [CrossRef]
31. Muir, C.D.; Hangarter, R.P.; Moyle, L.C.; Davis, P.A. Morphological and anatomical determinants of mesophyll conductance in wild relatives of tomato (Solanum sect. Lycopersicon, sect. Lycopersicoides; Solanaceae). *Plant Cell Environ.* **2014**, *37*, 1415–1426. [CrossRef]
32. Peralta, I.E.; Spooner, D.M. Classification of wild tomatoes: A review. *Kurtziana* **2000**, *28*, 45–54.
33. Chetelat, R.; Pertuze, R.; Faundez, L.; Graham, E.; Jones, C. Distribution, ecology and reproductive biology of wild tomatoes and related nightshades from the Atacama Desert region of northern Chile. *Euphytica* **2009**, *167*, 77–93. [CrossRef]
34. Palacio, S.; Azorín, J.; Montserrat-Martí, G.; Ferrio, J.P. The crystallization water of gypsum rocks is a relevant water source for plants. *Nat. Commun.* **2014**, *5*, 4660. [CrossRef]
35. Martín-Gómez, P.; Barbeta, A.; Voltas, J.; Peñuelas, J.; Dennis, K.; Palacio, S.; Dawson, T.E.; Ferrio, J.P. Isotope-ratio infrared spectroscopy: A reliable tool for the investigation of plant-water sources? *New Phytol.* **2015**, *207*, 914–927. [CrossRef]
36. Dongmann, G.; Nurnberg, H.W.; Forstel, H.; Wagener, K. On the enrichment of $H_2{}^{18}O$ in the leaves of transpiring plants. *Radiat. Environ. Biophys.* **1974**, *11*, 41–52. [CrossRef]

37. Farquhar, G.D.; Richards, R.A. Isotopic Composition of Plant Carbon Correlates With Water-Use Efficiency of Wheat Genotypes. *Funct. Plant Biol.* **1984**, *11*, 539–552. [CrossRef]
38. Loucos, K.E.; Simonin, K.A.; Barbour, M.M. Leaf hydraulic conductance and mesophyll conductance are not closely related within a single species. *Plant Cell Environ.* **2017**, *40*, 203–215. [CrossRef]
39. Kahmen, A.; Simonin, K.; Tu, K.; Goldsmith, G.R.; Dawson, T.E. The influence of species and growing conditions on the 18-O enrichment of leaf water and its impact on 'effective path length'. *New Phytol.* **2009**, *184*, 619–630. [CrossRef]
40. Holloway-Phillips, M.; Cernusak, L.A.; Barbour, M.; Song, X.; Cheesman, A.; Munksgaard, N.; Stuart-Williams, H.; Farquhar, G.D. Leaf vein fraction influences the Péclet effect and ^{18}O enrichment in leaf water. *Plant Cell Environ.* **2016**, *39*, 2414–2427. [CrossRef]
41. Farquhar, G.D.; Gan, K.S. On the progressive enrichment of the oxygen isotopic composition of water along leaves. *Plant Cell Environ.* **2003**, *26*, 801–819. [CrossRef]